

Group-based optimization of potent and cell-active inhibitors of the von Hippel-Lindau (VHL) E3 ubiquitin ligase: structure-activity relationships leading to the chemical probe VH298

Pedro Soares[†], Morgan S. Gadd[†], Julianty Frost^{†‡}, Carles Galdeano[†], Lucy Ellis[†], Ola Epemolu[†], Sonia Rocha[‡], Kevin D. Read[†], Alessio Ciulli^{†*}

[†]Division of Biological Chemistry and Drug Discovery, School of Life Sciences, University of Dundee, Dow Street, Dundee, DD1 5EH, Scotland, UK. [‡]Center for Gene Regulation and Expression, School of Life Sciences, University of Dundee, Dow Street, Dundee, DD1 5EH, Scotland, UK.

Supporting Information

Table of Contents

S2 - Supplementary Figures

S11 – FP Competition Assay Data

S22 – ITC Data

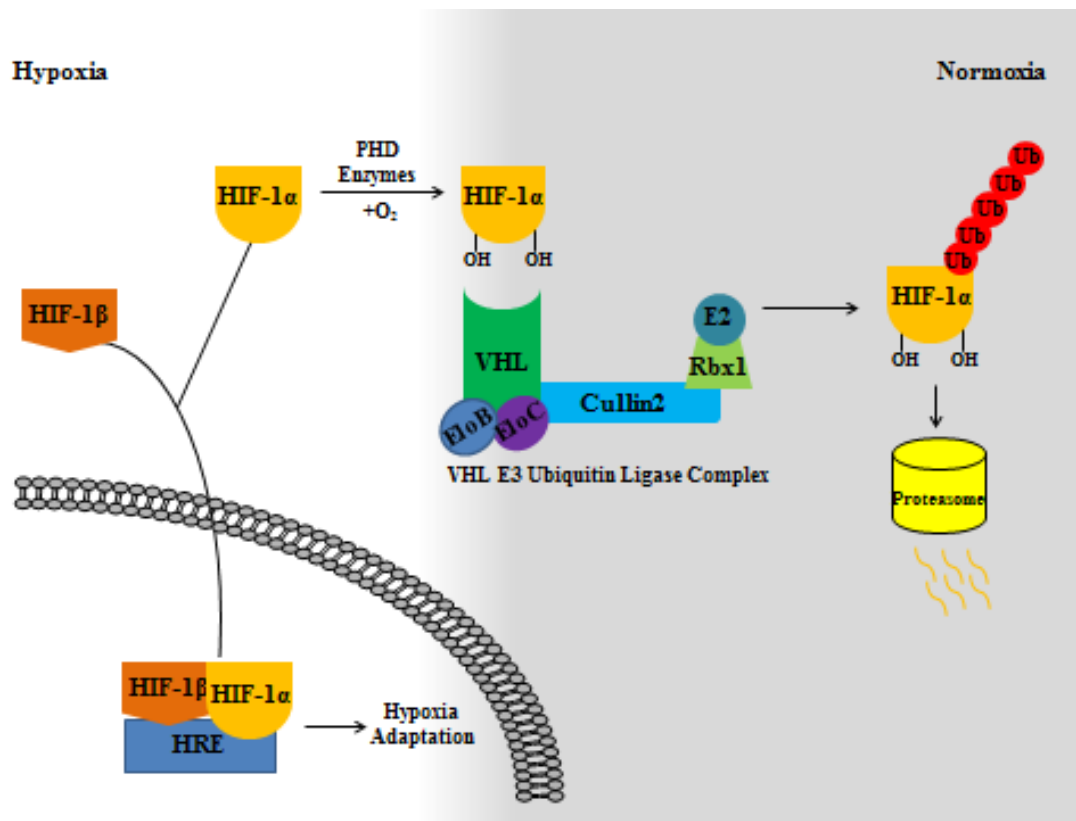
S26 – SPR Data

S30 – Evaluation of VHL inhibitors intracellular accumulation

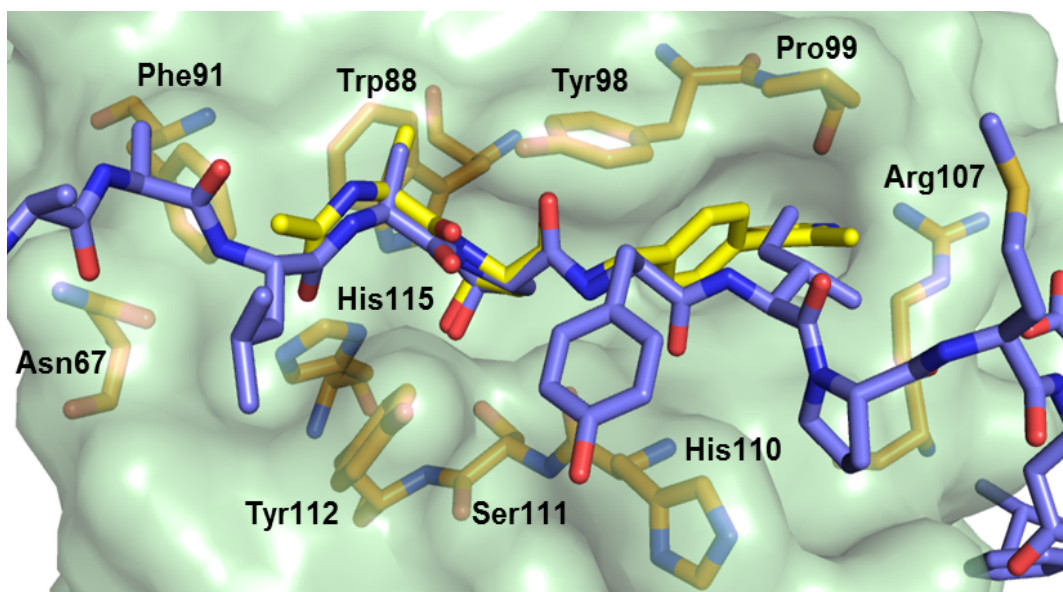
S31 – X-ray Crystallography Data Processing and Refinement Statistics

S33 – ¹H and ¹³C NMR spectra

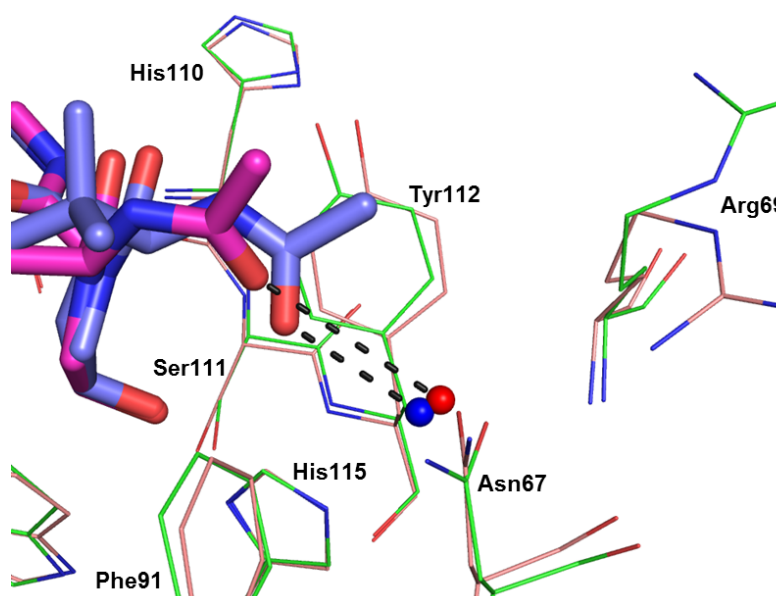
Supplementary Figures



Supplementary Figure 1. Under normoxia conditions, HIF-1 α is hydroxylated, recognized by the CRL2^{VHL} complex, poly ubiquitinated and target for hydrolysis by the proteasome. Under hypoxia conditions, HIF-1 α dimerizes with HIF-1 β forming a transcriptionally active complex that binds to Hypoxia Response Elements, promoting hypoxia adaptation.

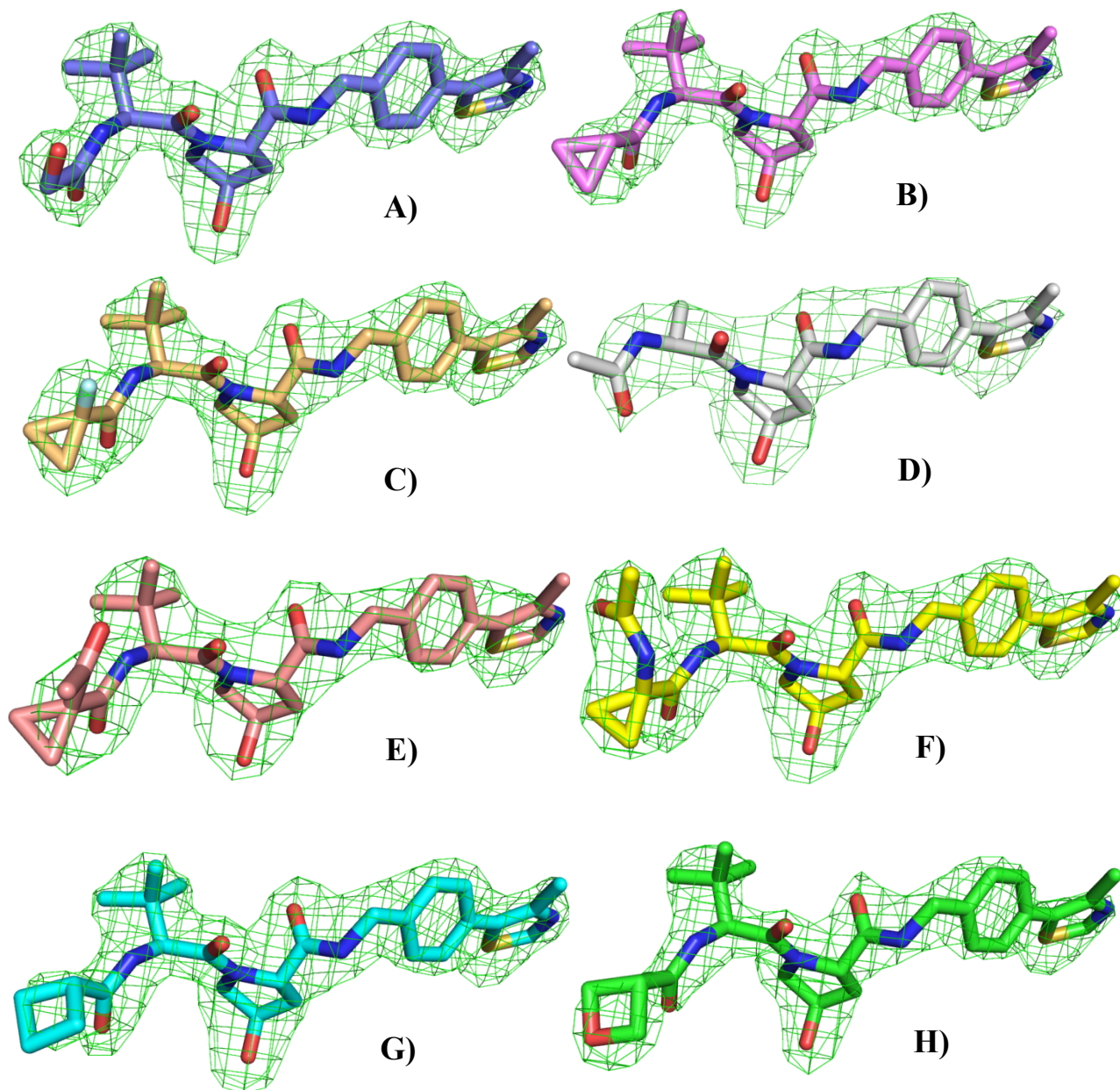


Supplementary Figure 2. Crystal structure of VBC in complex with HIF-1 α peptide (purple carbons PDB 4AJY) and inhibitor **11** (yellow carbons). VHL is shown as a pale green surface and the VHL residues forming the binding pocket as orange stick representations.

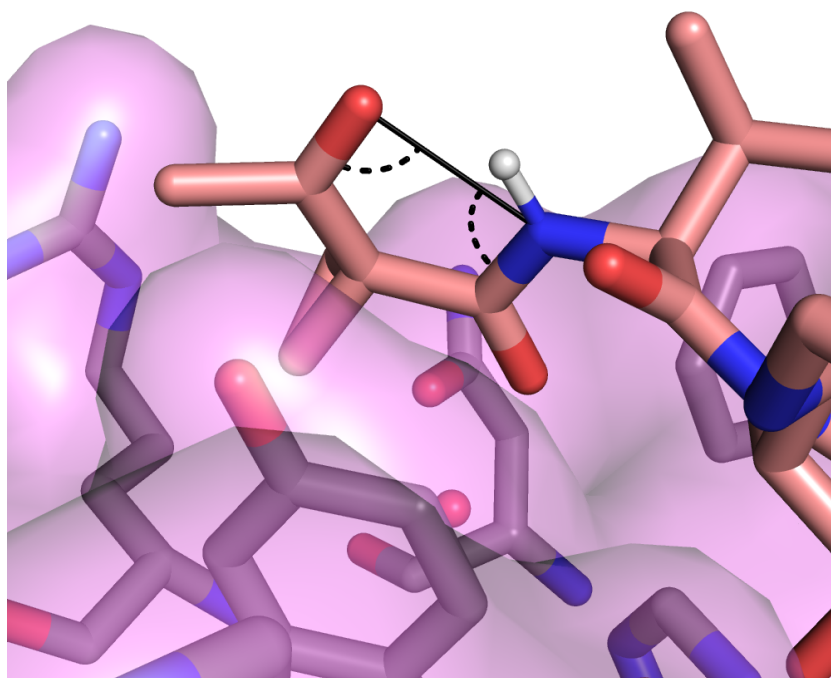


Supplementary Figure 3. Crystal structure of VBC in complex with inhibitor **VH032** (purple carbons PDB 4W9H) and inhibitor **11** (pink carbons). Residues forming the LHS of VHL pocket are shown as line representations (pink carbons **VH032** structure and green carbons inhibitor **11** structure). The structural water at the LHS is shown as a red sphere in

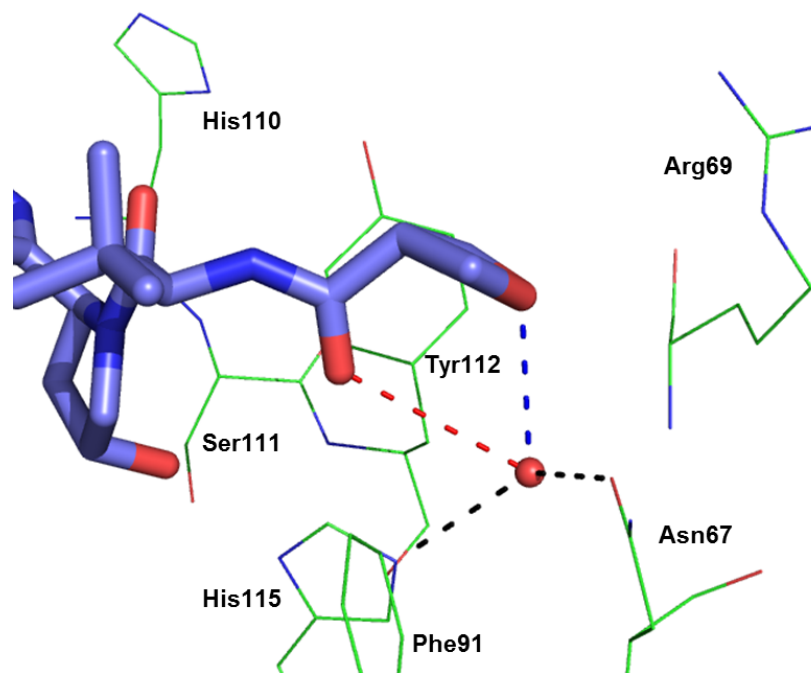
inhibitor **11** structure and as a blue sphere in **VH032** structure. Distances between inhibitors LHS carbonyl and respective structural waters are shown as black dashed lines.



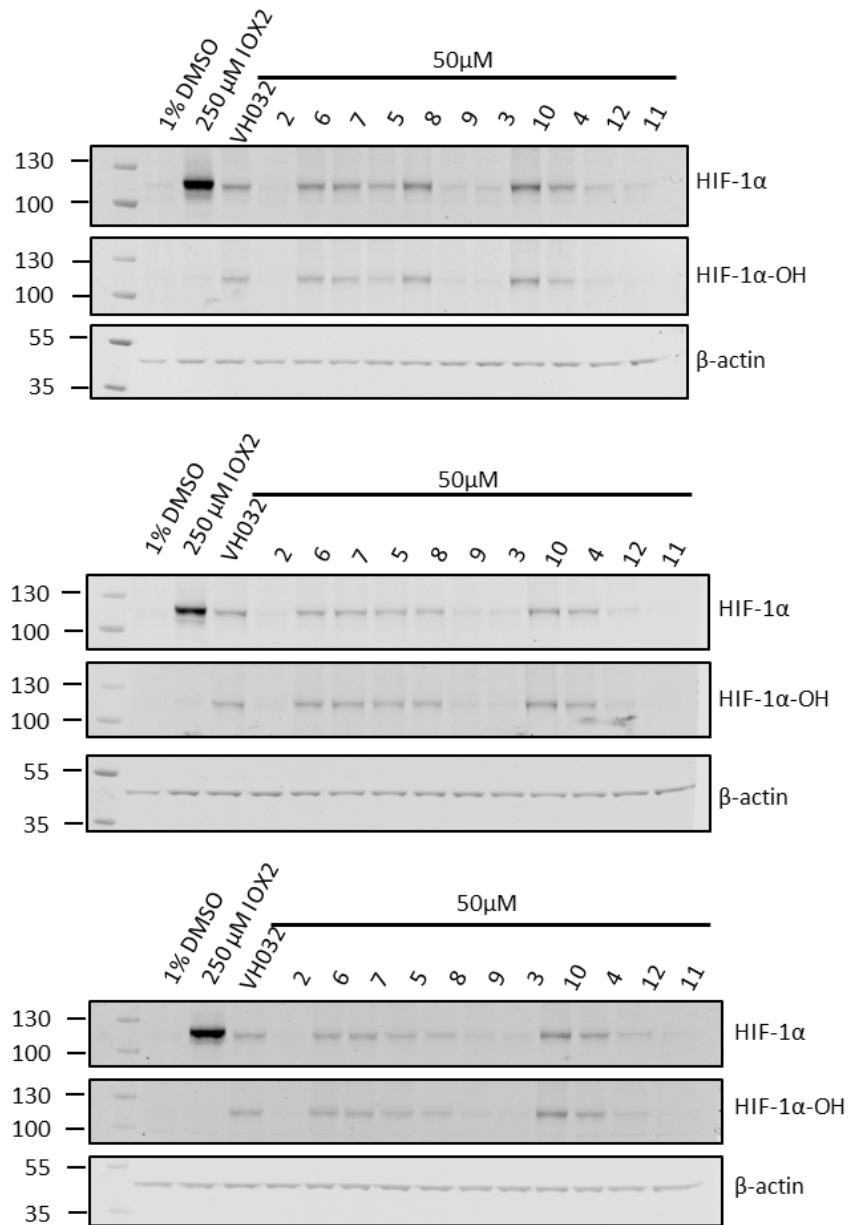
Supplementary Figure 4. Electron density at ligand binding sites. Ligands A) **3**; B) **6**; C) **10**; D) **11**; E) **16**; F) **17**; G) **18**; H) **19** shown as sticks bound to the complex of VBC (not shown). An omit map ($F_o - F_c$) is shown in green contoured at 3σ around each modelled ligand with a carve radius of 1.6 \AA .



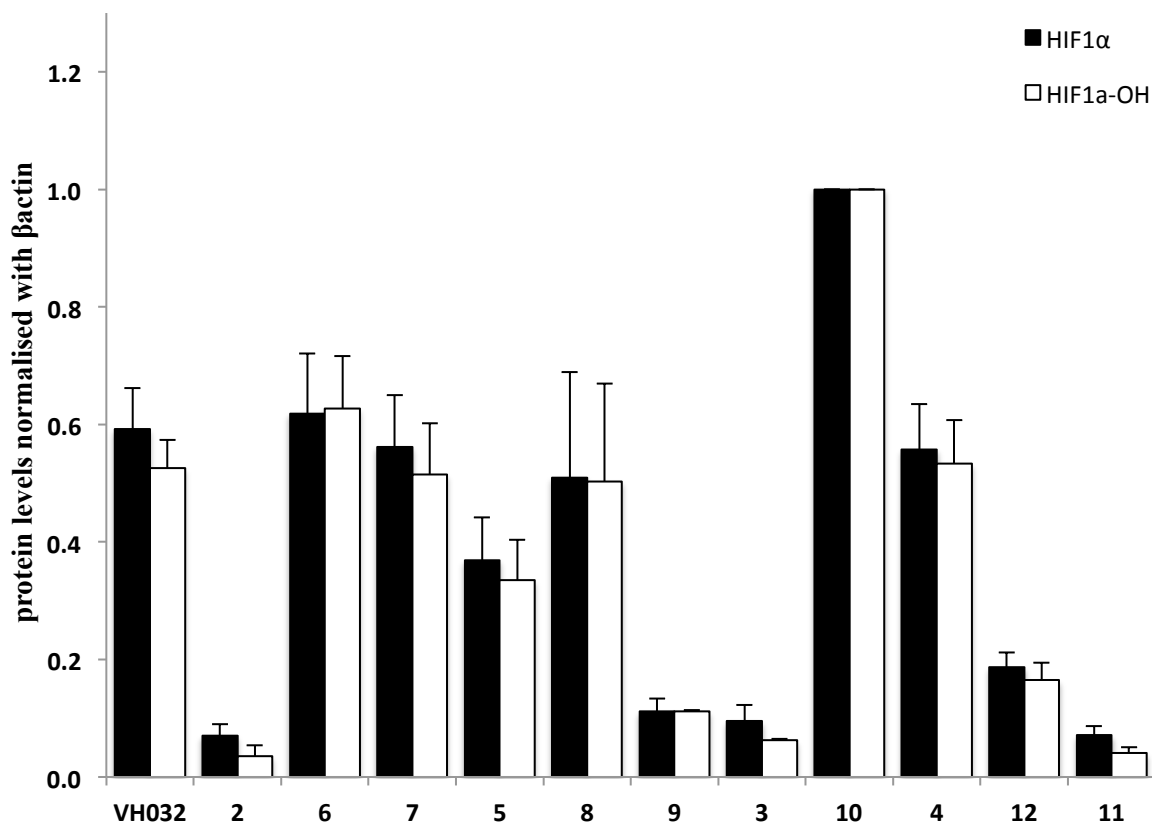
Supplementary Figure 5. Crystal structure of VBC in complex with inhibitor **16** (pink carbons). VHL is shown as purple pale surface and residues forming the LHS of VHL pocket are shown grey stick representation. Structural water is shown as a red sphere. Distance and angles are shown as black continuous and dashed lines respectively.



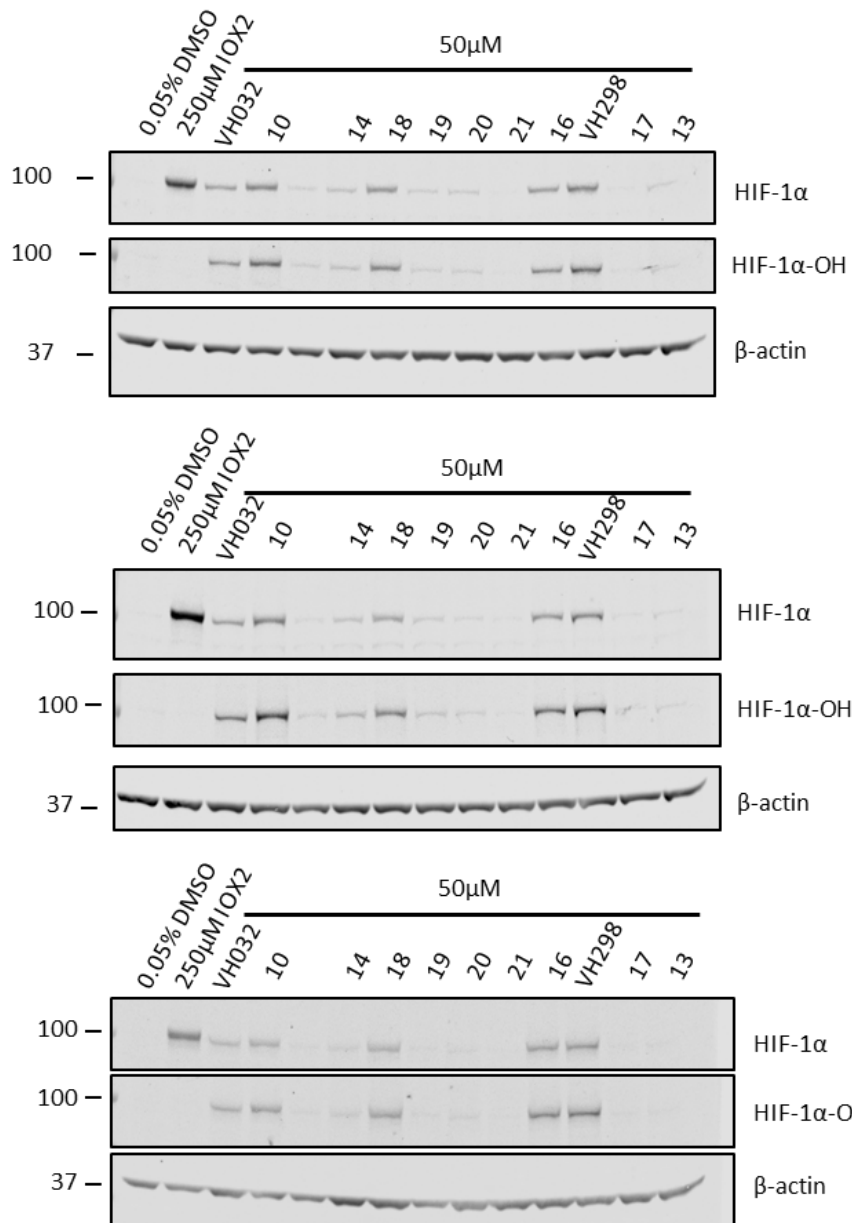
Supplementary Figure 6. Crystal structure of VBC in complex with inhibitor **19** (purple carbons). Residues forming the LHS of VHL pocket are shown as line representations (green carbons). The structural water at the LHS is shown as a red sphere. Distances between inhibitor oxygen of oxetane and inhibitor LHS amide carbonyl with structural water are shown as blue and red dashed lines respectively. Distances between structural water and residues on the LHS of the pocket are shown as black dashed lines



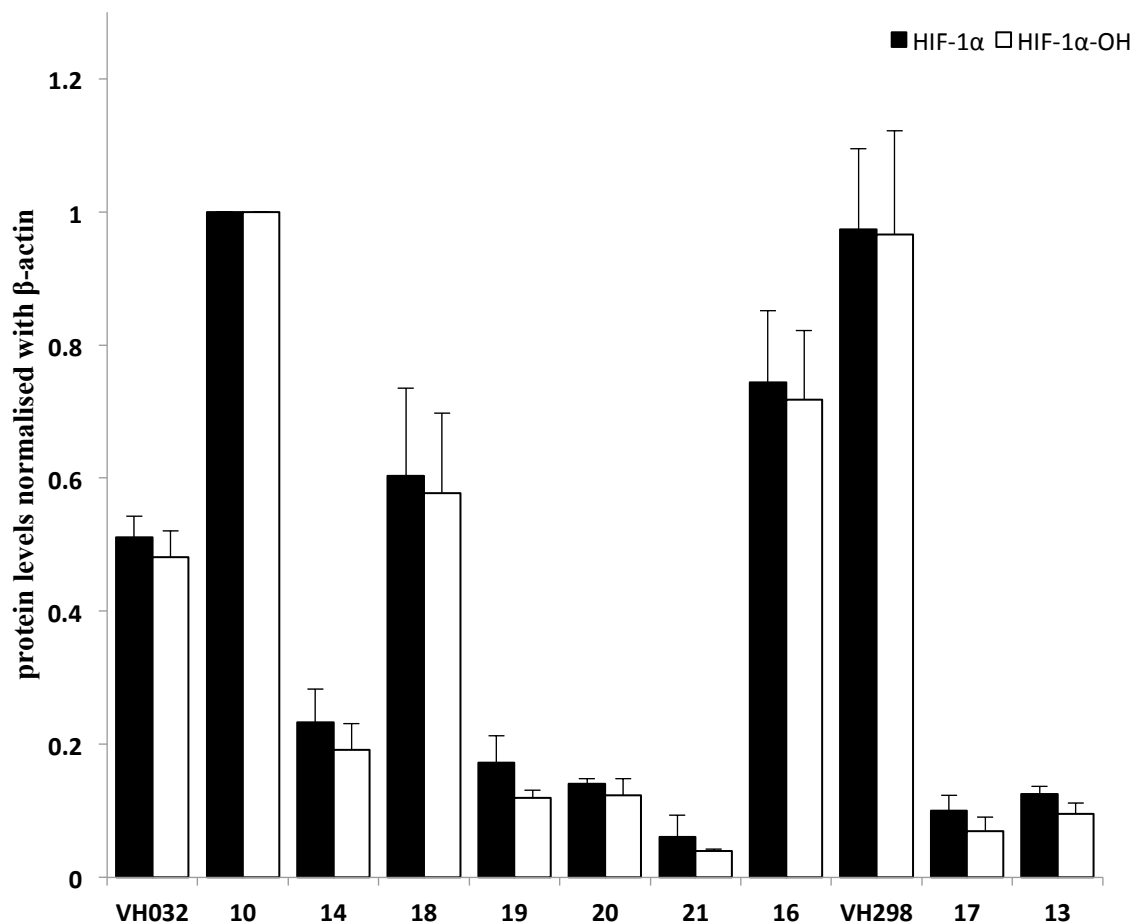
Supplementary Figure 7. Immunoblots of HIF- α subunits in HeLa cells treated with 50 μ M of VHL inhibitors **VH032** and **2-12**; 1% DMSO, 250 μ M IOX2 for 2h.



Supplementary Figure 8. Quantification of HIF-1 α stabilization levels in HeLa cells for compounds **VH032** and **2–12** measured by Western Blot (SI Figure 7) after 2h treatment. The assay was performed in triplicate; protein levels were normalized to β -actin levels and are reported as mean \pm st. dev. relative to compound **10**. IOX2 was used as positive control and cells treated with DMSO vehicle were used as negative control.

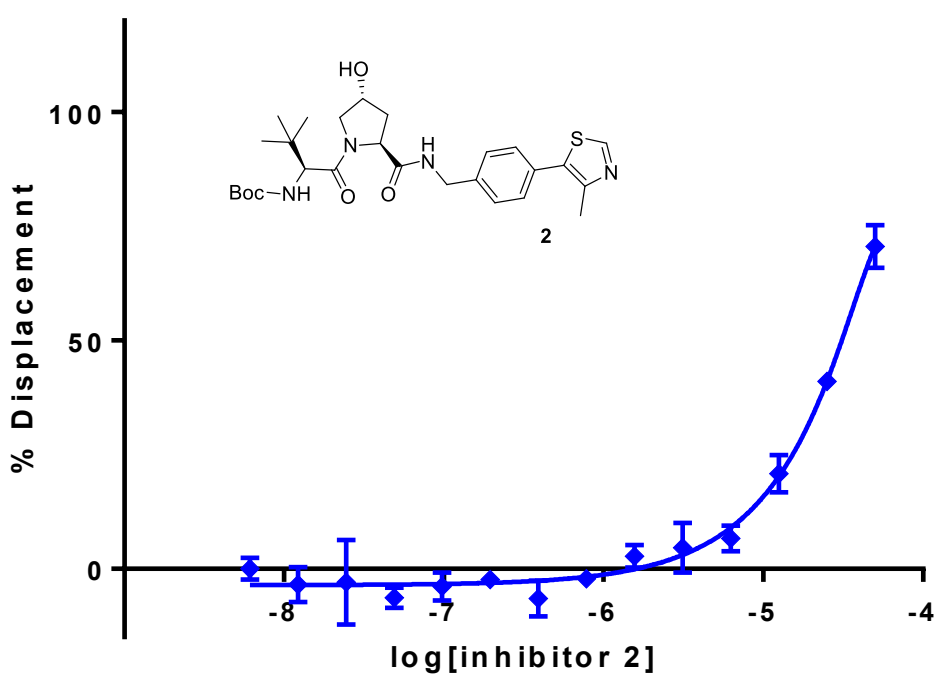
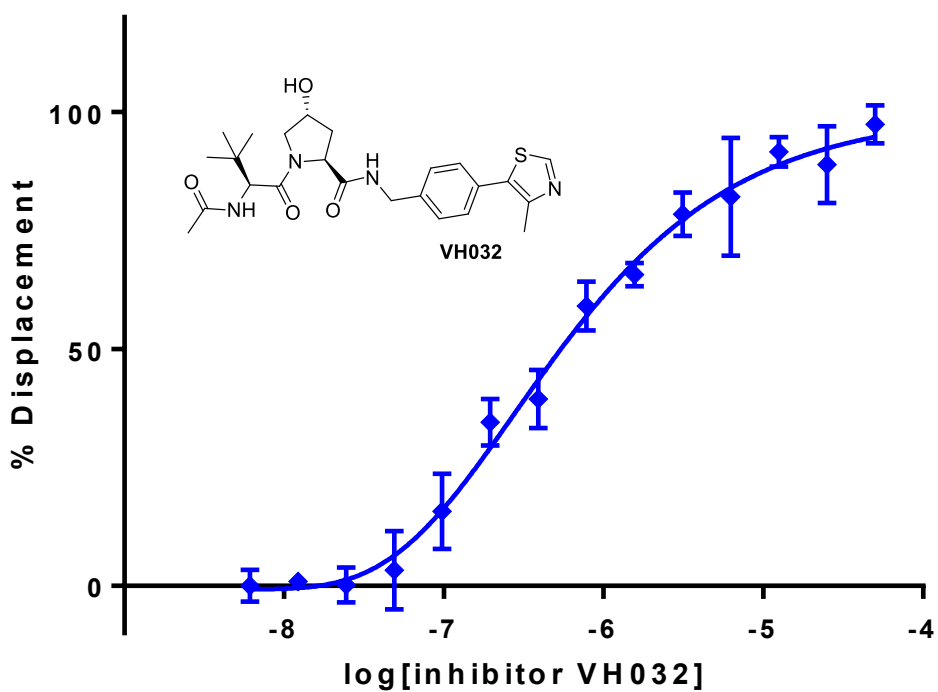


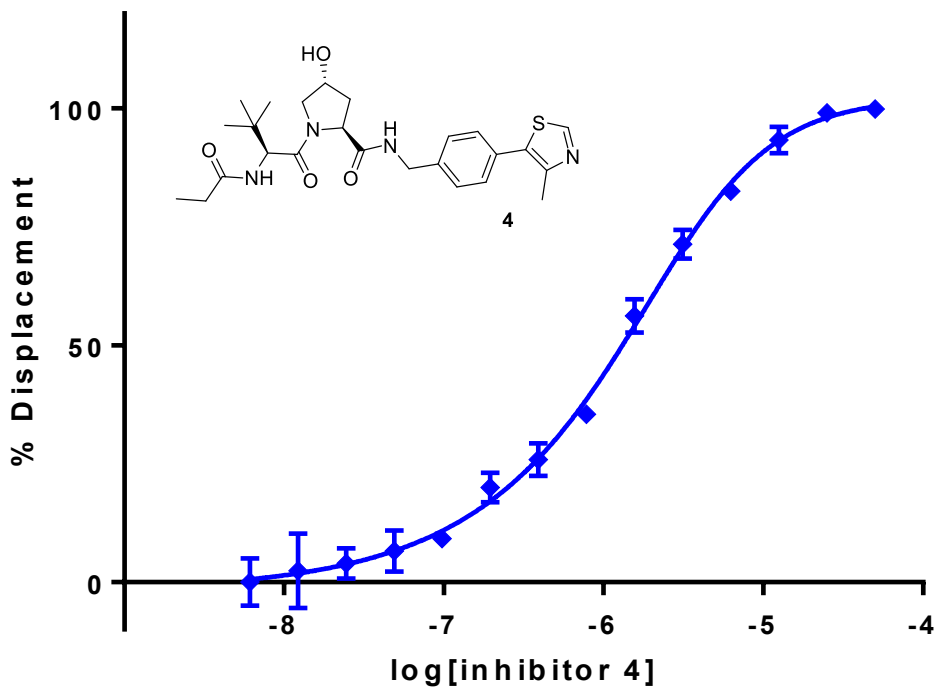
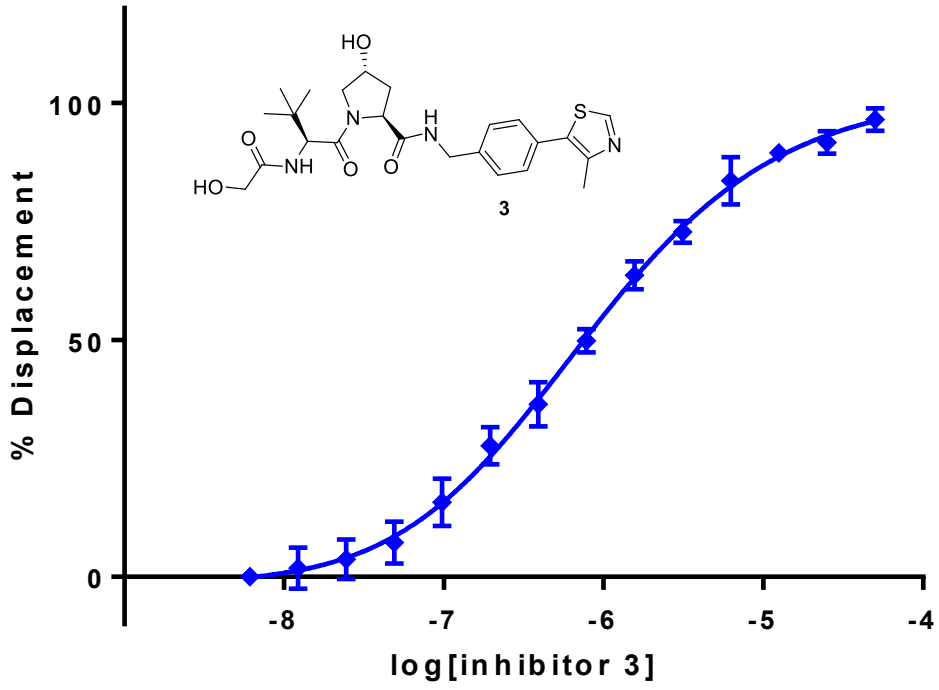
Supplementary Figure 9. Immunoblots of HIF- α subunits in HeLa cells treated with 50 μ M of VHL inhibitors **VH032, 10, 13, 14, VH298, 16-21**; 1% DMSO, 250 μ M IOX2 for 2h.

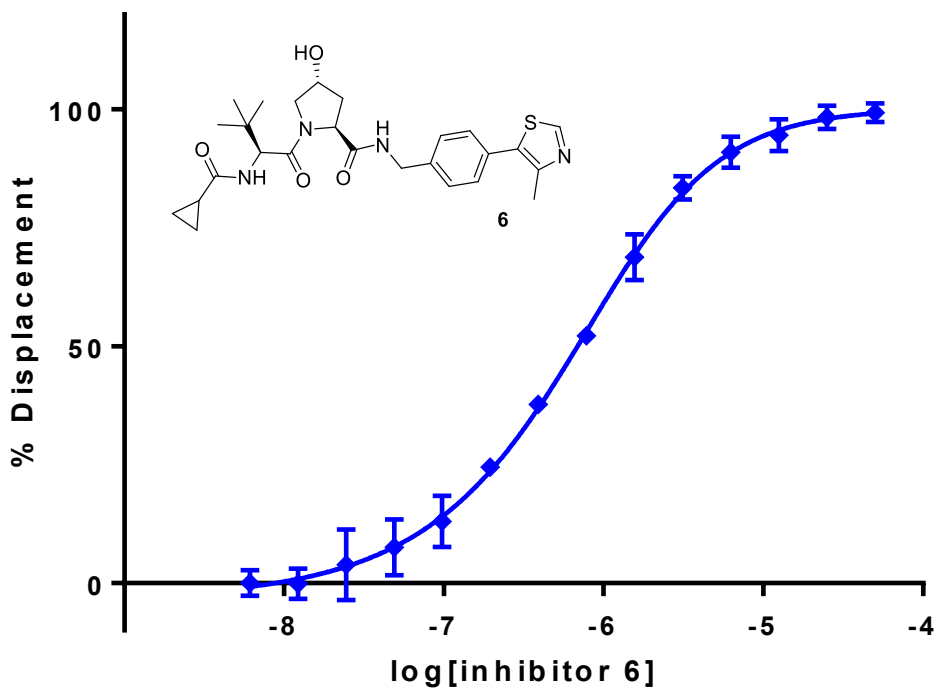
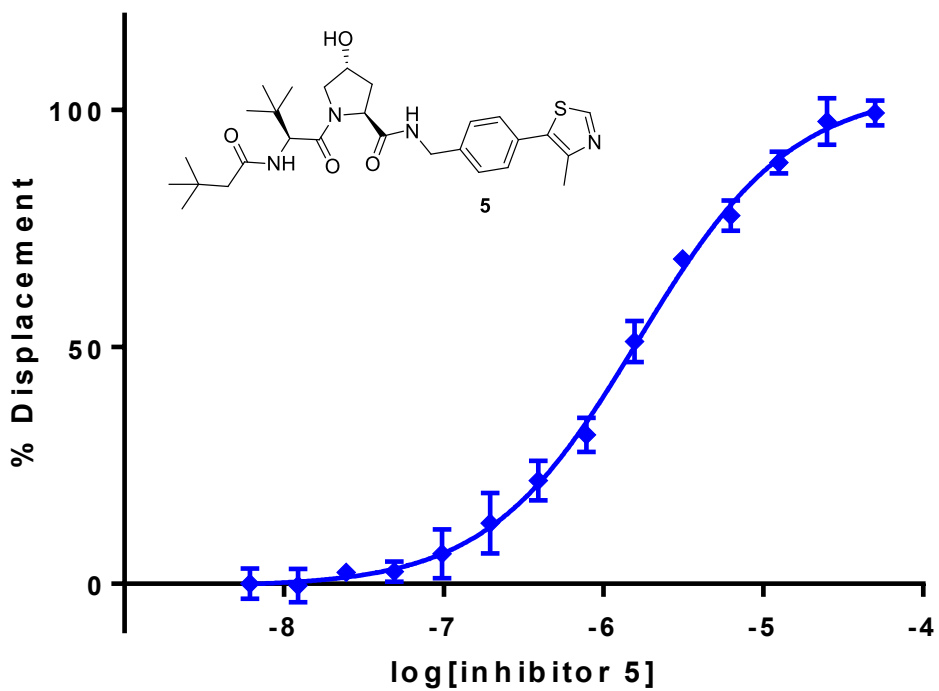


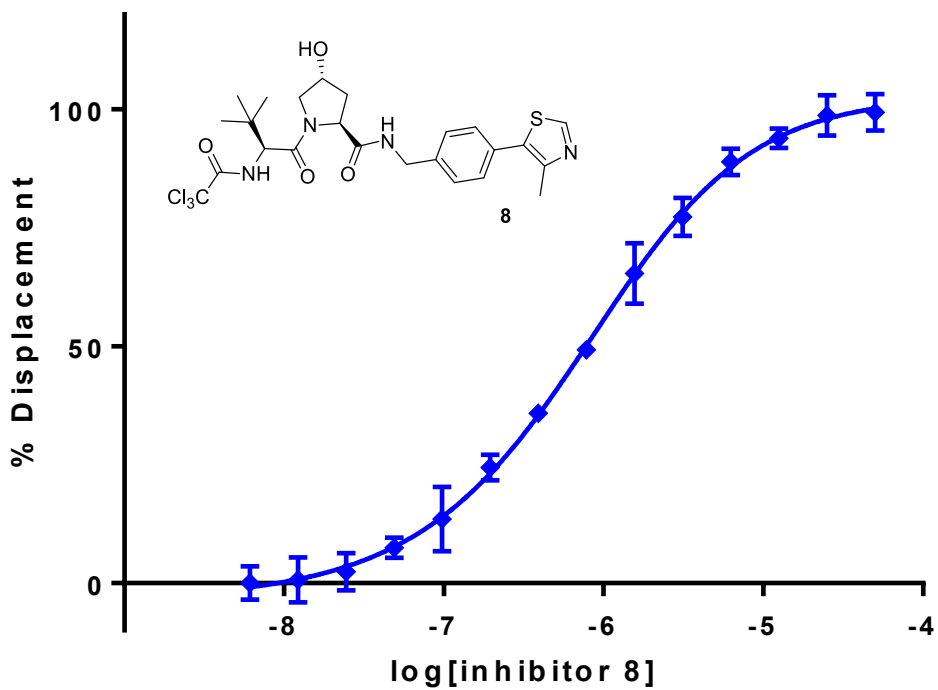
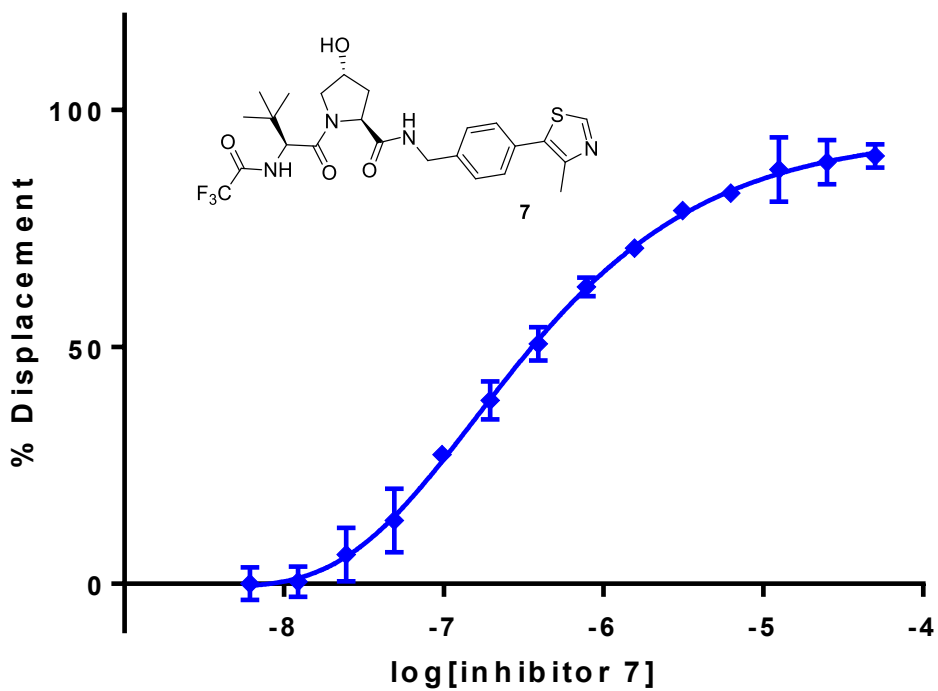
Supplementary Figure 10. Quantification of HIF-1 α stabilization levels in HeLa cells for compounds VH032, VH298, 10 and 13-21 measured by Western Blot (SI Figure 9) after 2h treatment. The assay was performed in triplicate; protein levels were normalized to β -actin levels and are reported as mean \pm st. dev. relative to compound **10**. IOX2 was used as positive control and cells treated with DMSO vehicle were used as negative control.

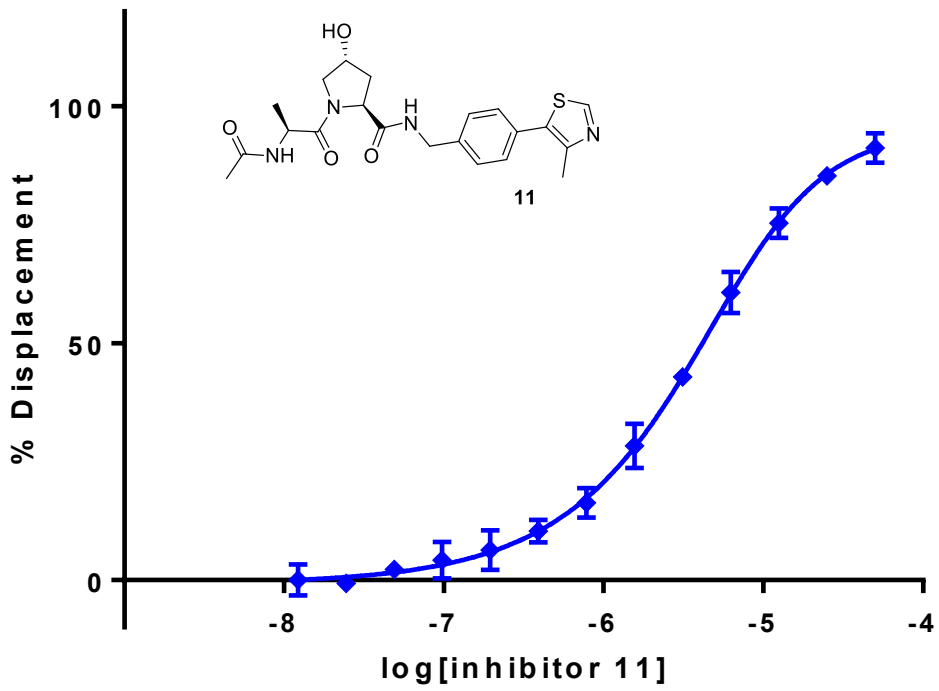
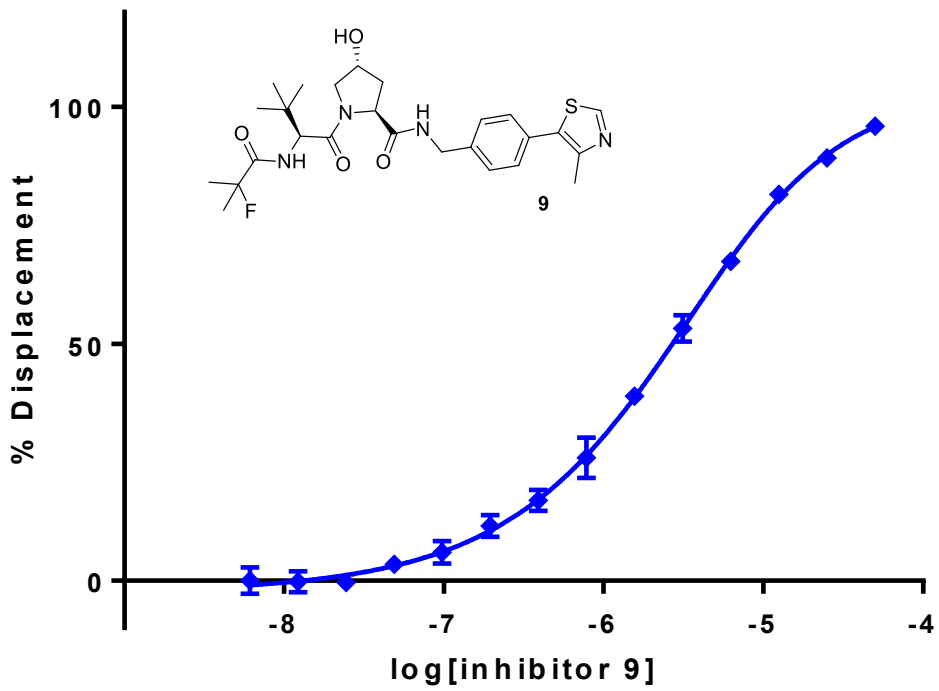
Florescence Polarization Competition Assay Graphs

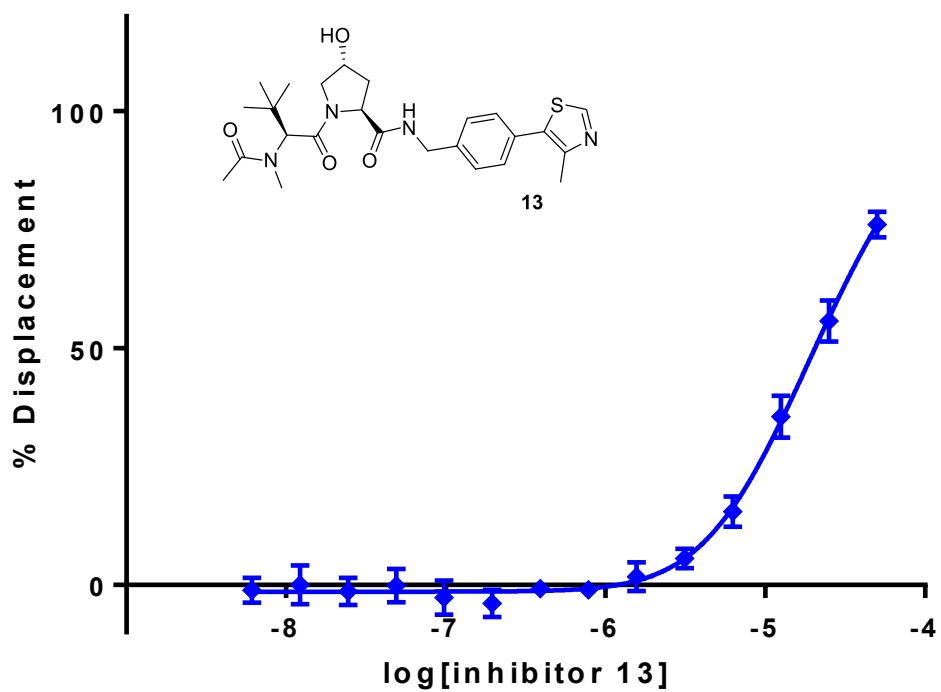
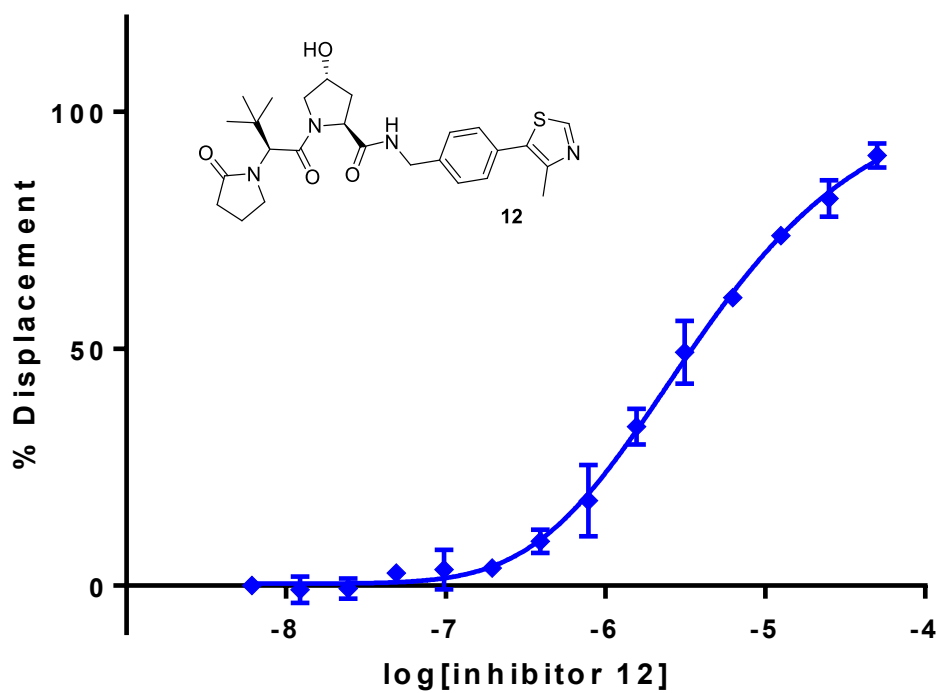


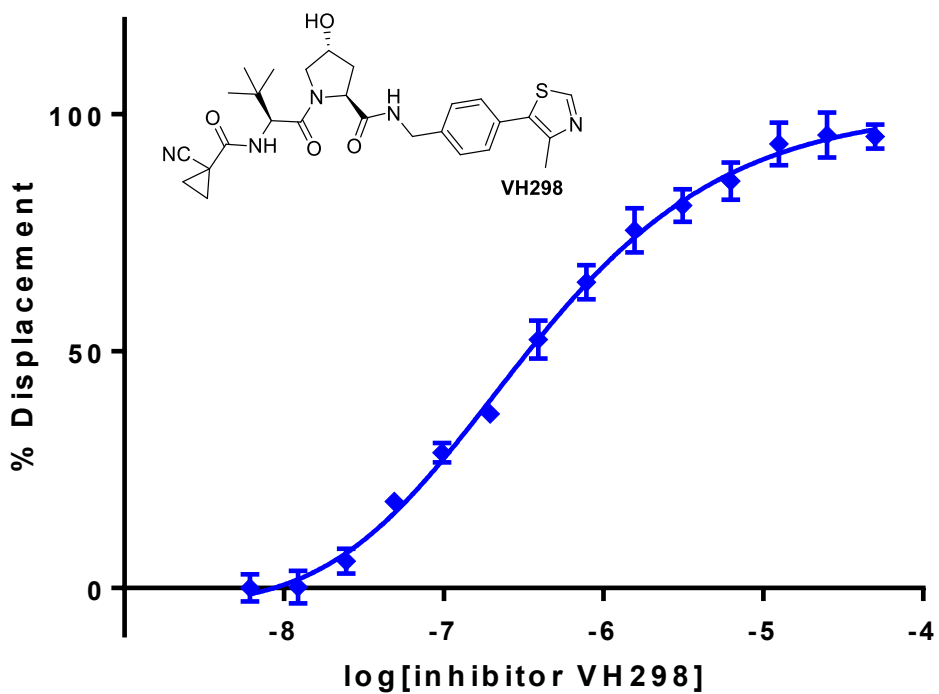
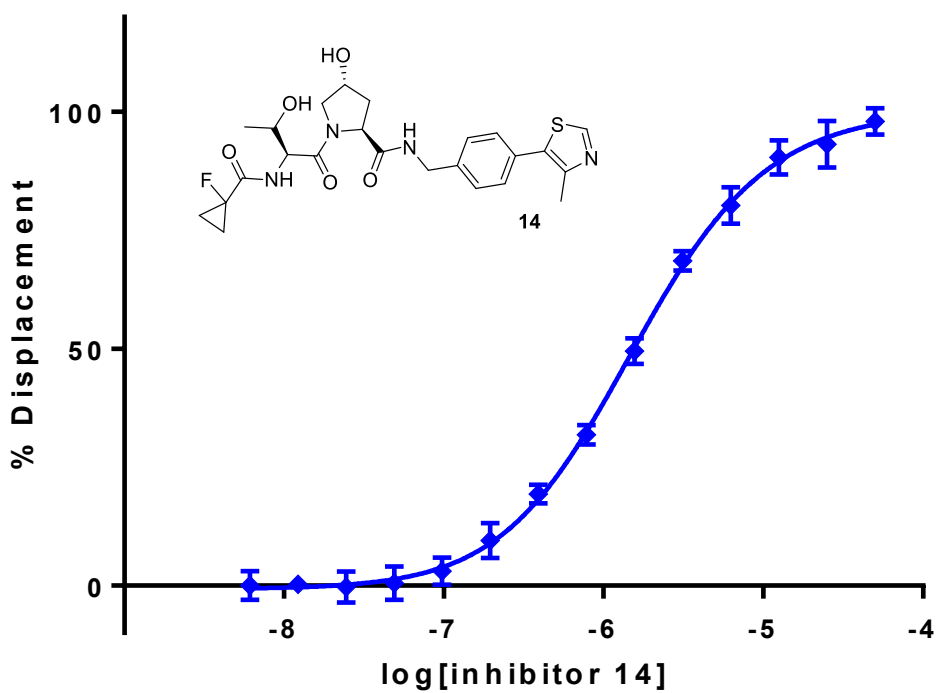


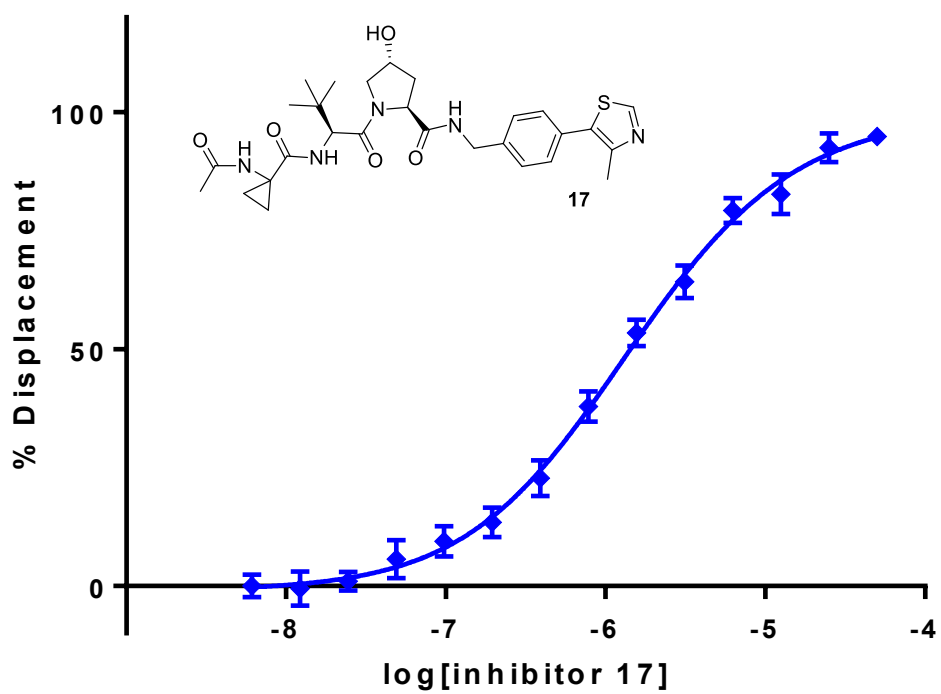
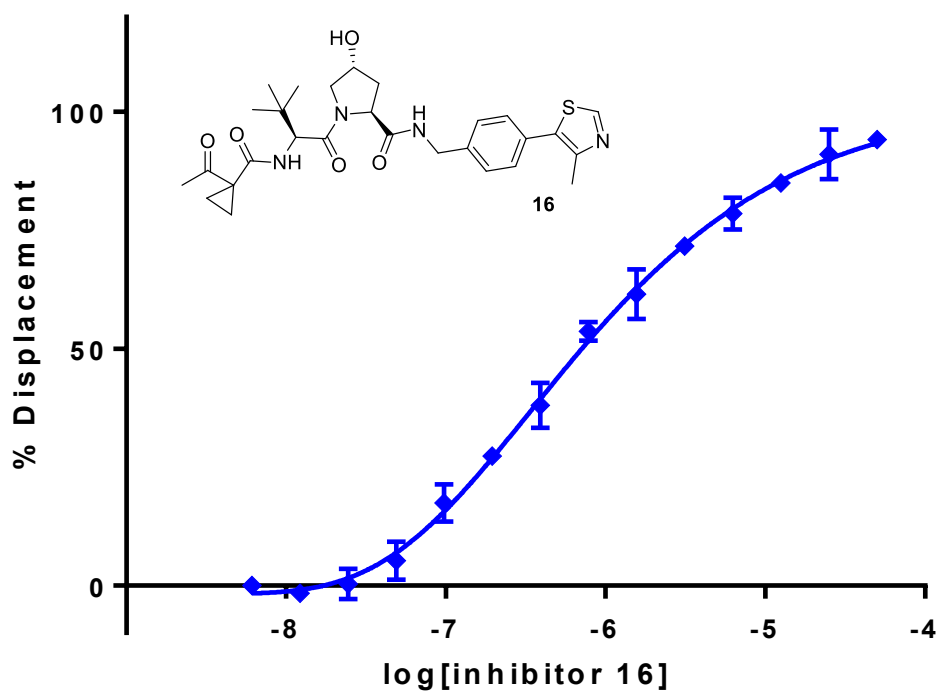


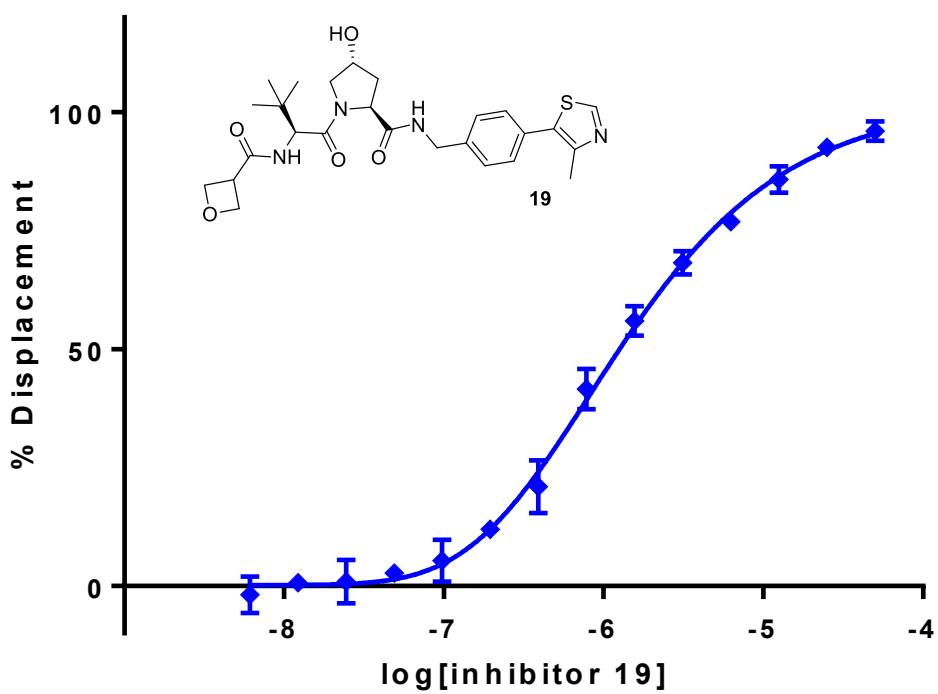
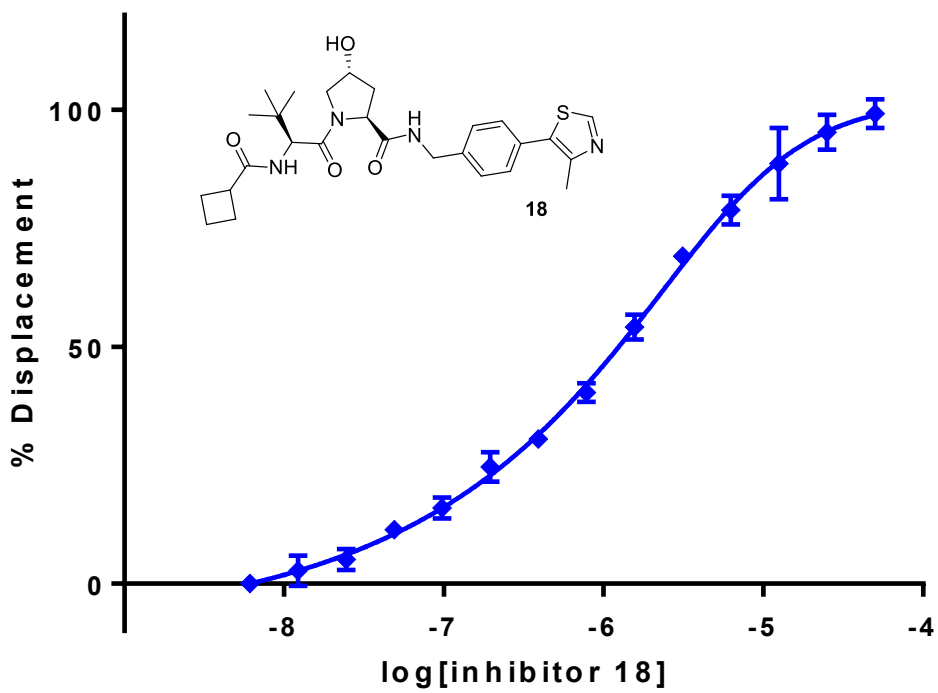


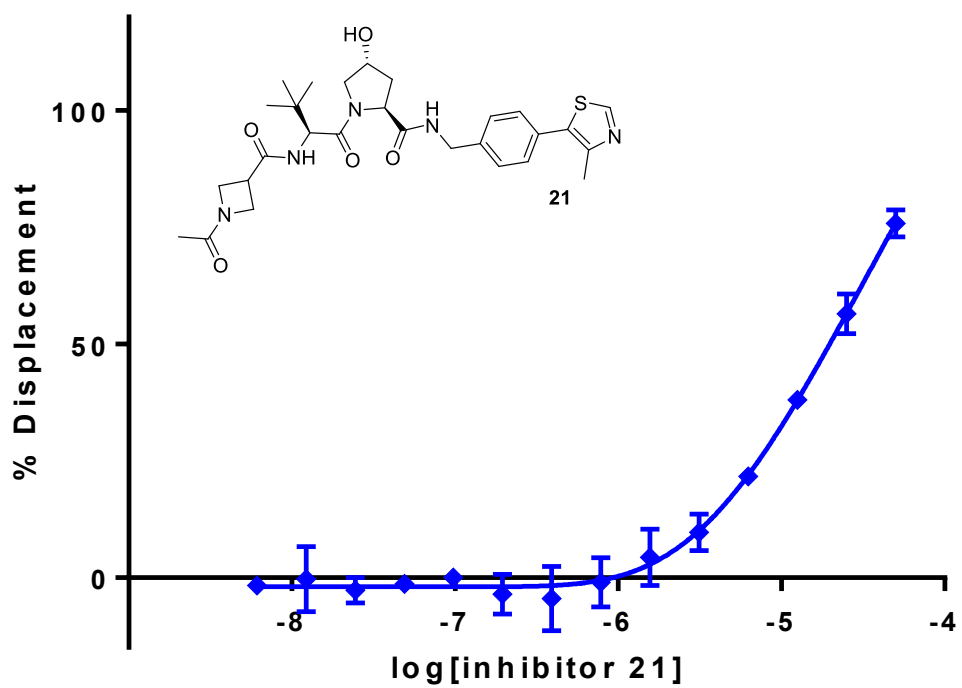
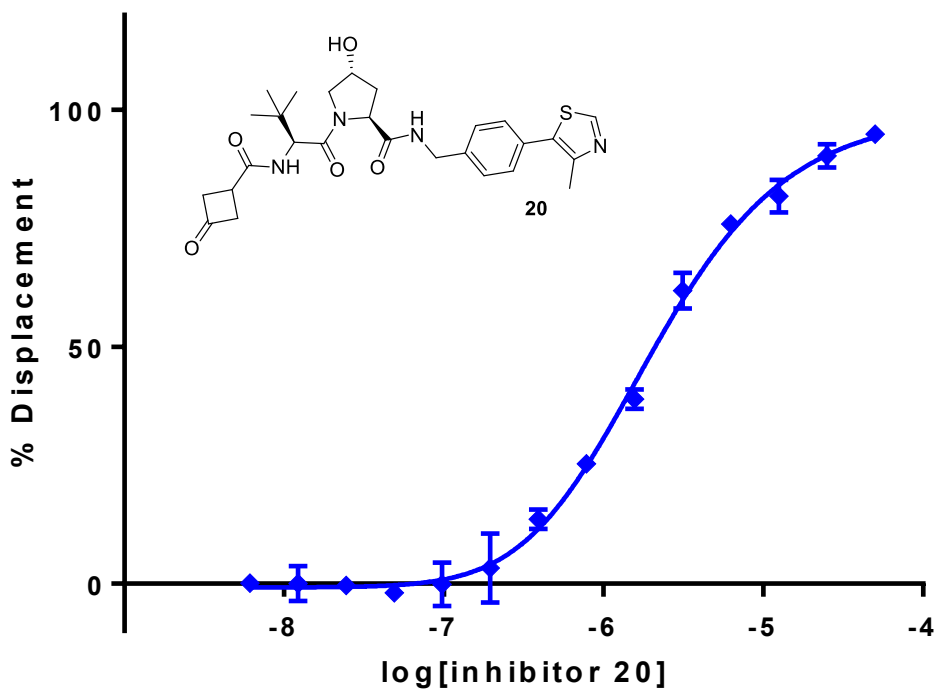




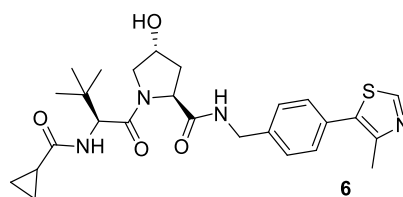
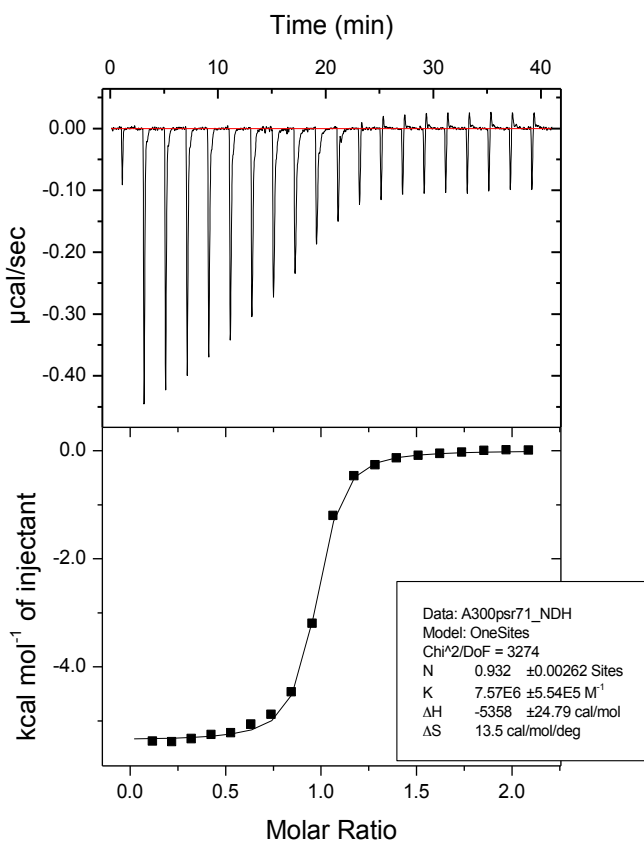
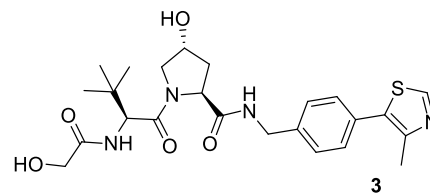
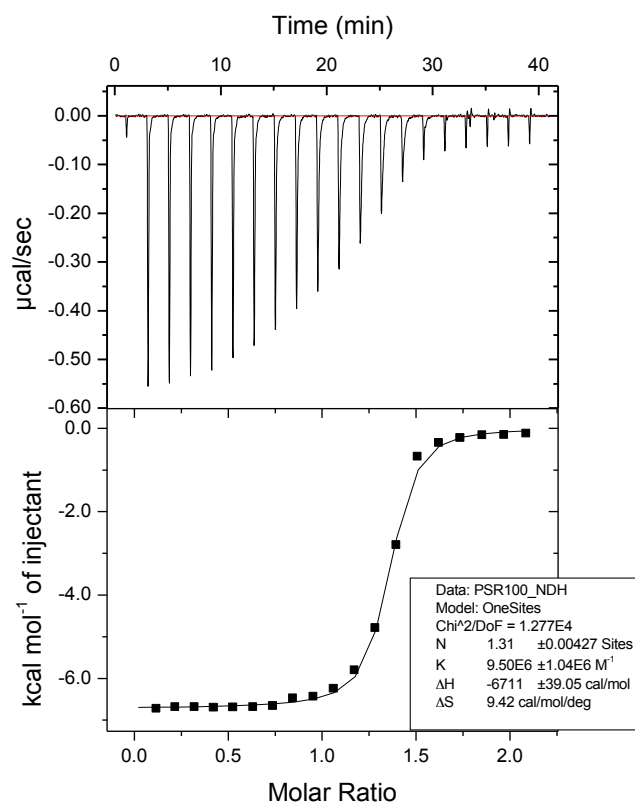


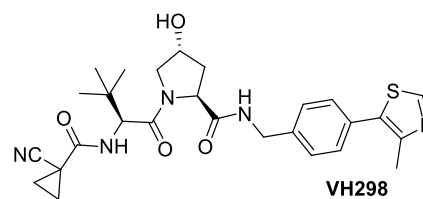
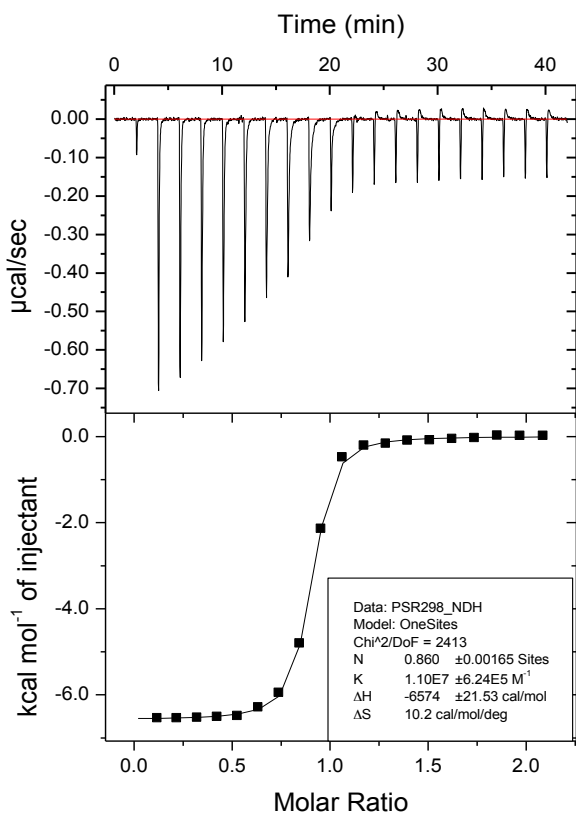
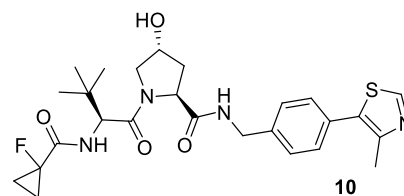
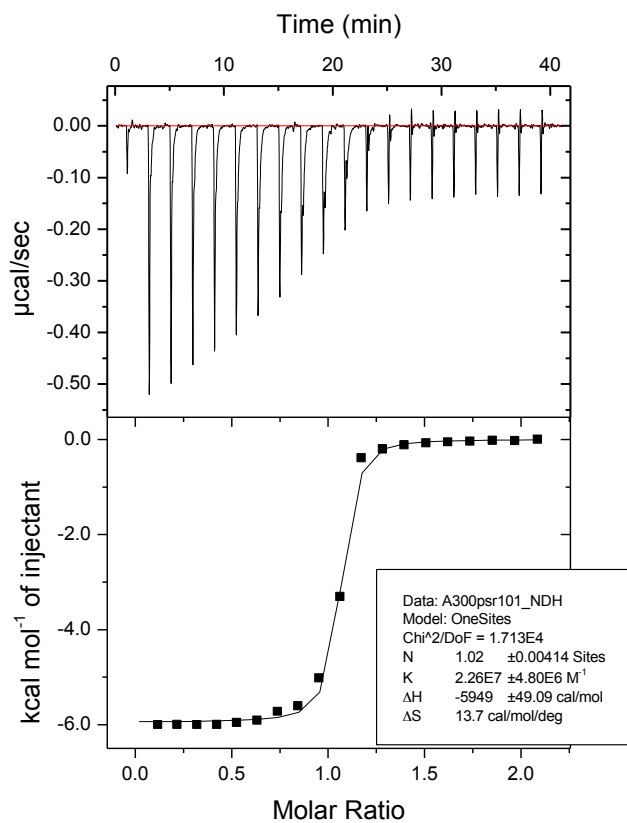


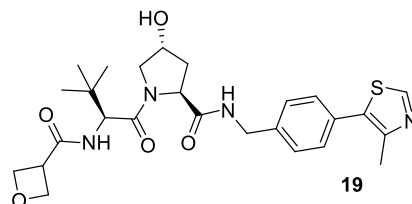
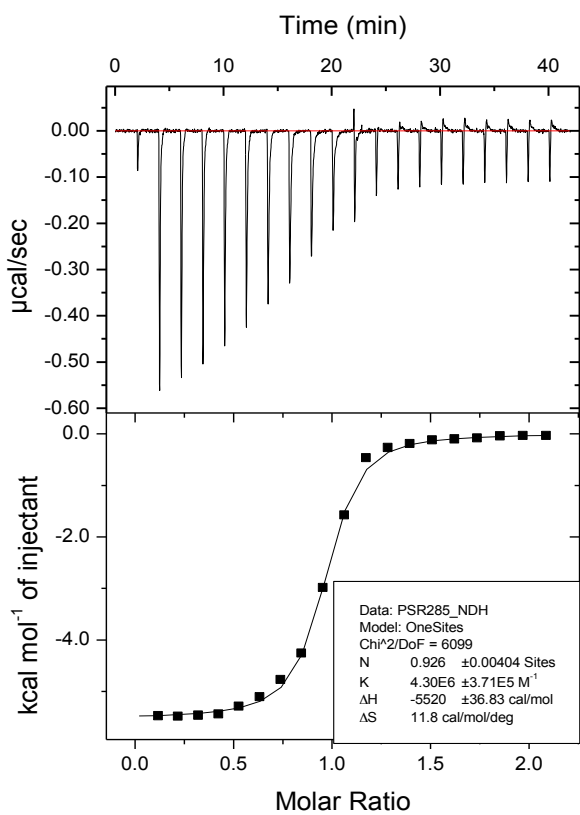
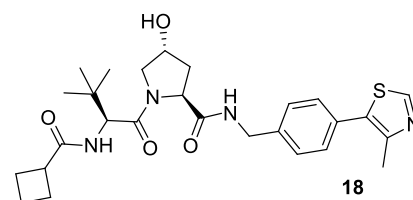
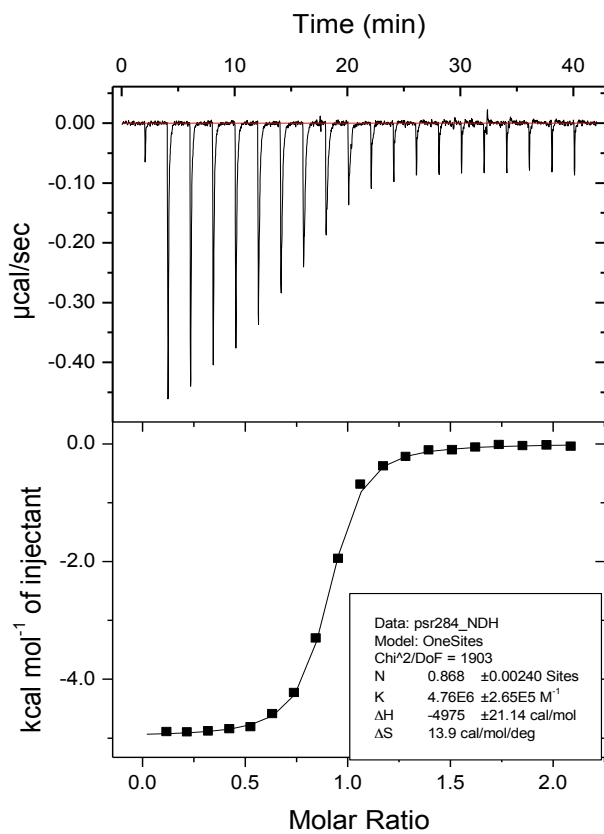




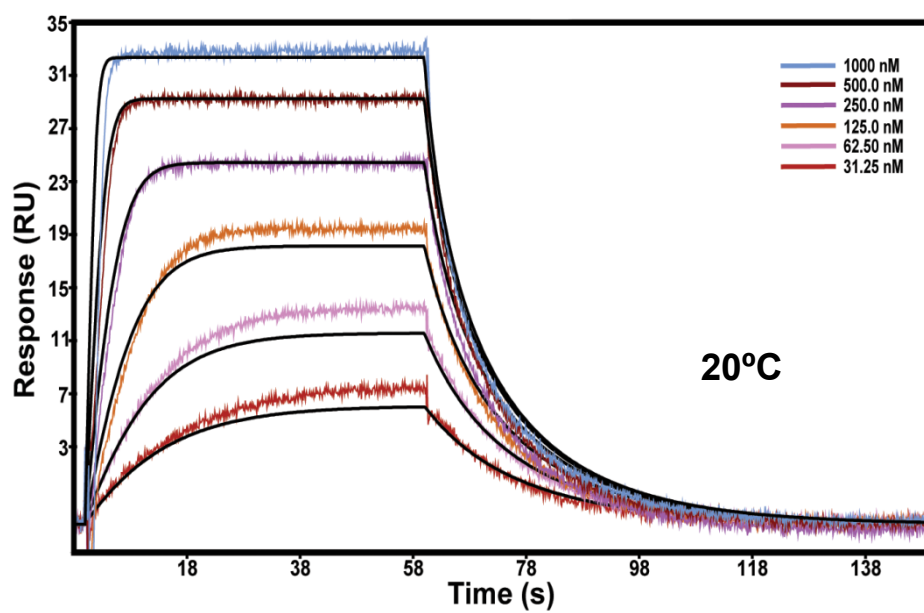
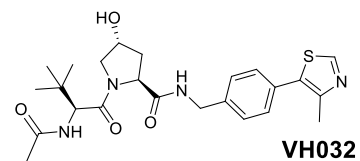
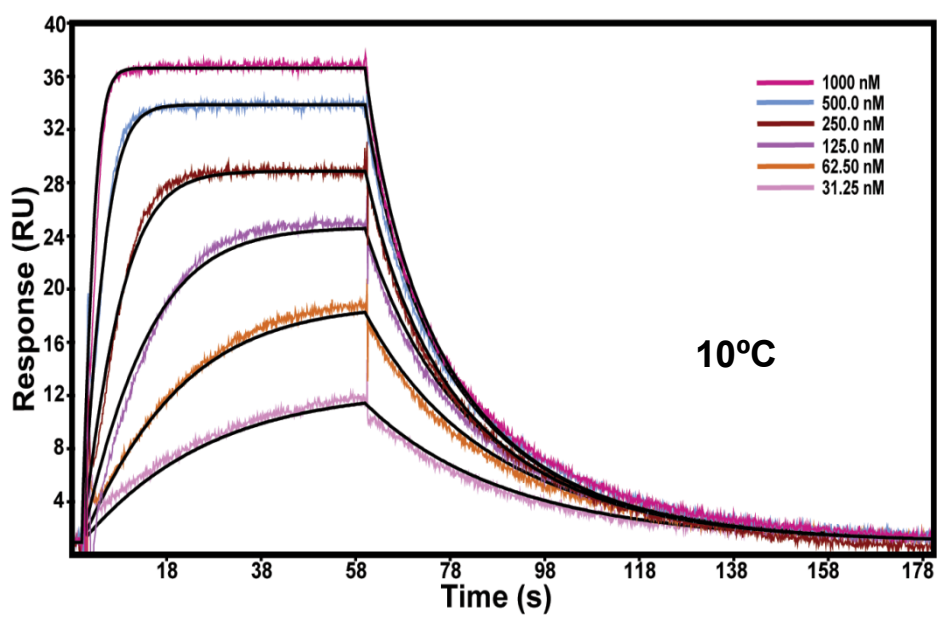
ITC Titrations

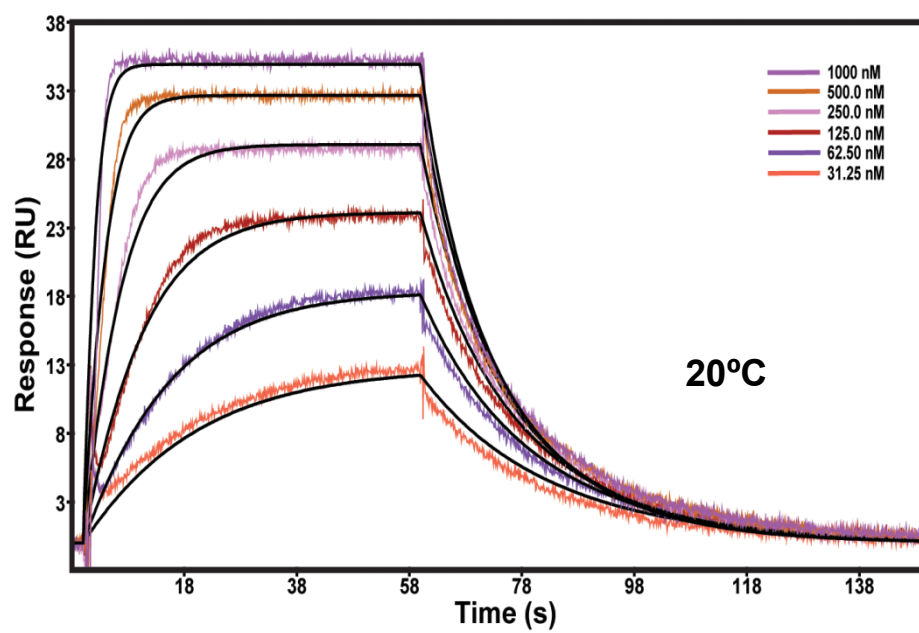
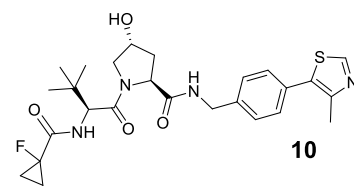
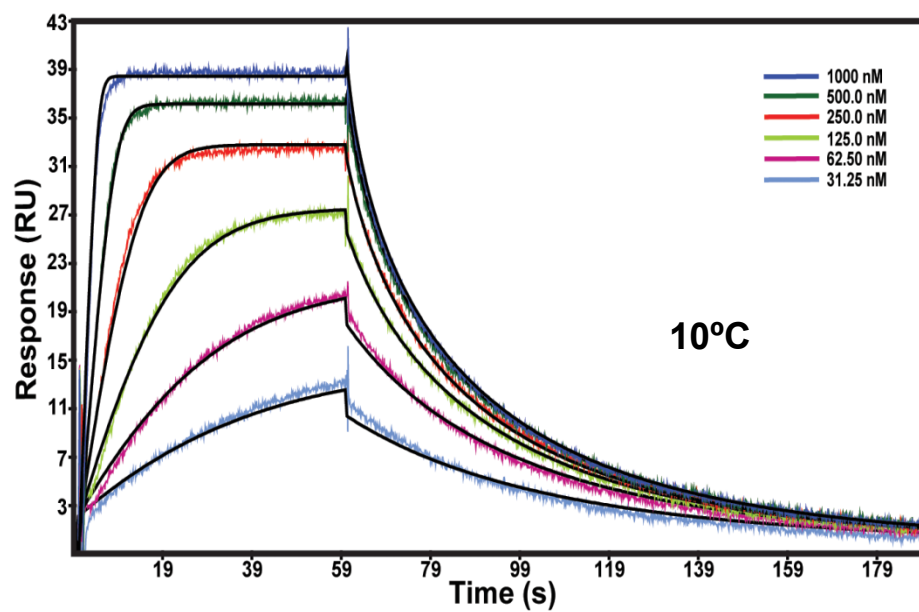


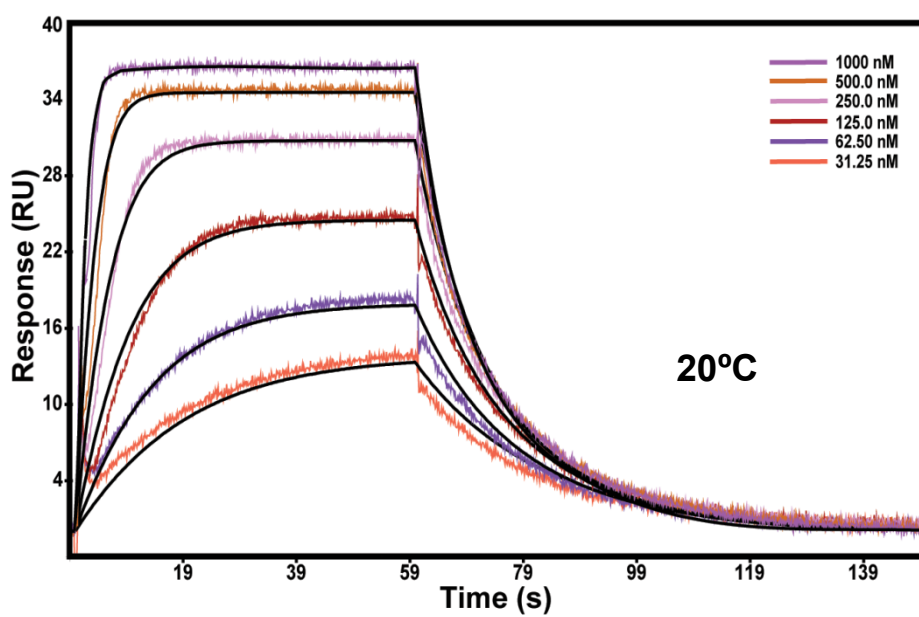
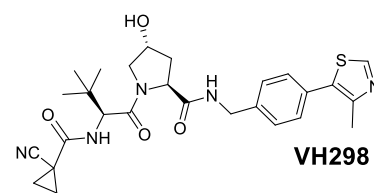
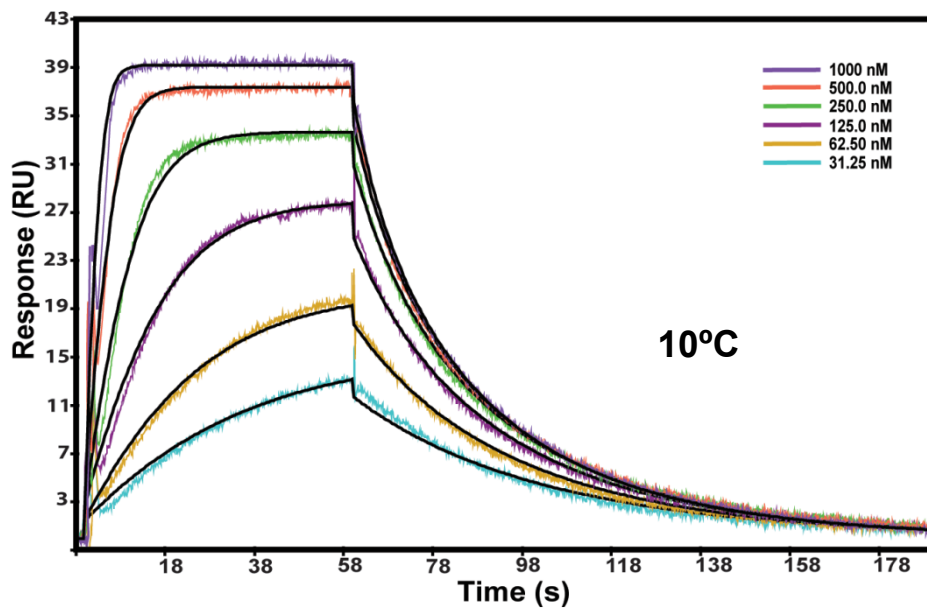


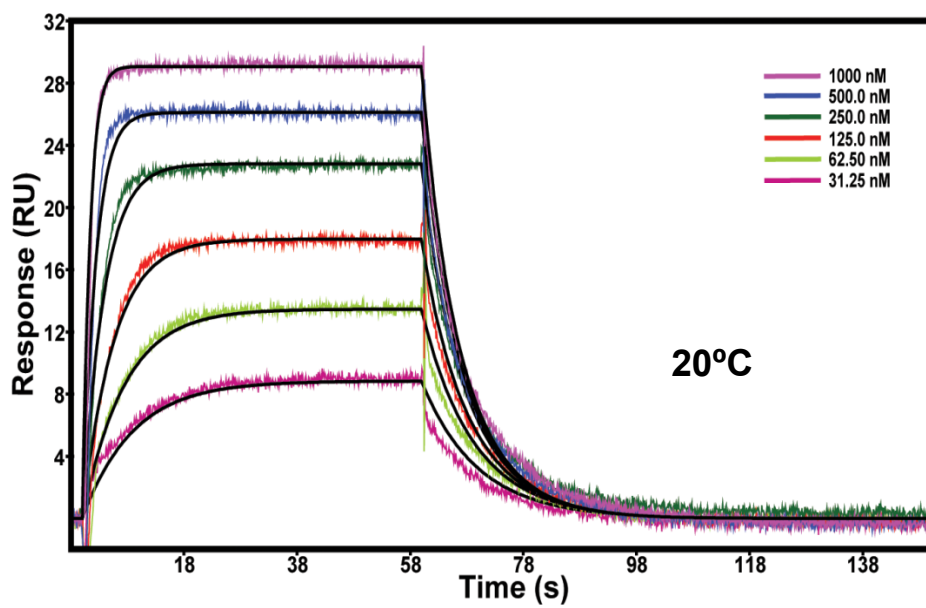
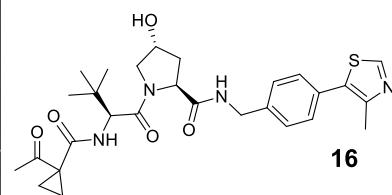
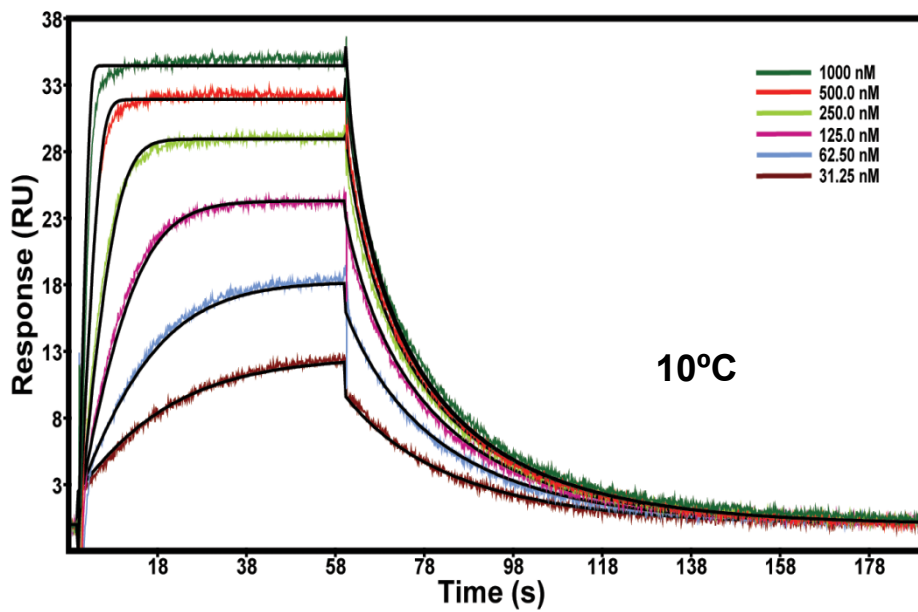


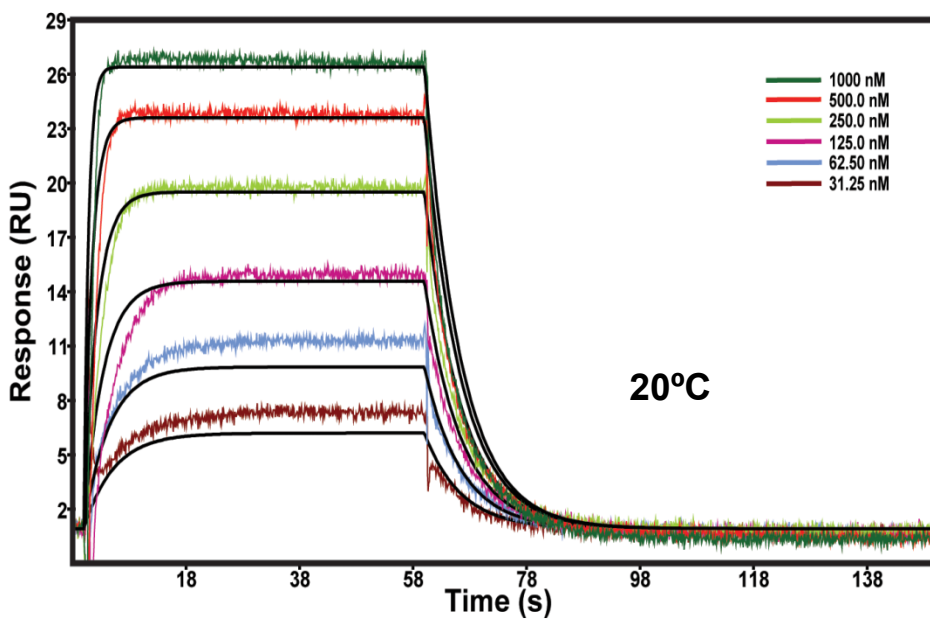
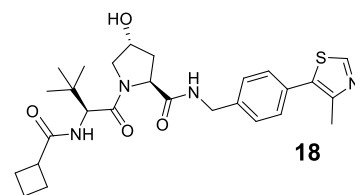
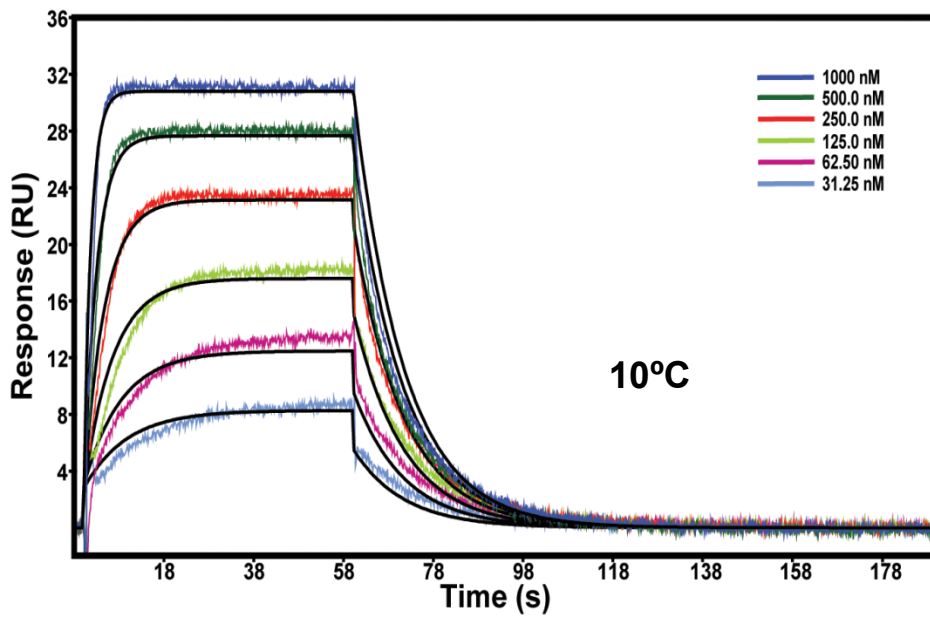
SPR Sensograms











X-ray Crystallography

Supplementary Table 1

Evaluation of intracellular accumulation of VHL inhibitors **VH032**, **10**, **VH298**, **16** and **18** on HeLa cells after 2 h treatment with compounds.

Inhibitor	Compound associated with cells (μM)	Fraction unbound (fu)	Final free compound concentration in cells (μM)
VH032	463.8	0.0016	0.742
10	383.6	0.0002	0.071
VH298	150.0	0.0007	0.058
16	100.0	0.0008	0.046
18	204.0	0.0008	0.093

Propranolol compound with high concentration associated with cells (2679.0 μM) and Metoprolol compound with high fraction unbound (0.0050) were used as controls for the experiment.

Supplementary Table 2.

Crystallographic data processing and refinement statistics.

Values in parentheses are for the highest resolution shell.

Dataset	Inhibitor 3	Inhibitor 6	Inhibitor 10	Inhibitor 11
Synchrotron	Diamond	Diamond	Diamond	Diamond
Wavelength (Å)	0.9174	0.9174	0.9174	0.9282
Processing statistics				
Space group	<i>P4₁22</i>	<i>P4₁22</i>	<i>P4₁22</i>	<i>P4₁22</i>
Unit cell parameters				
<i>a, b</i> (Å)	93.3	93.2	93.4	93.1
<i>c</i> (Å)	365.0	365.1	365.2	363.0
Resolution limits (Å)	48.9–2.10 (2.14–2.10)	48.9–2.20 (2.24–2.20)	49.0–2.20 (2.24–2.20)	48.8–2.90 (3.03–2.90)
Total reflections	849102 (41946)	556127 (31559)	540233 (25019)	311841 (39080)
Unique reflections	95188 (4654)	82957 (4452)	83072 (4446)	36661 (4375)
Completeness (%)	99.8 (99.9)	99.8 (100)	99.6 (99.0)	100 (100)
Multiplicity	8.9 (9.0)	6.7 (7.1)	6.5 (5.6)	8.5 (8.9)
<i>R</i> _{merge} (%)	14.2 (98.0)	14.1 (85.7)	10.4 (72.2)	21.2 (89)
<i>I</i> / σ (<i>I</i>)	9.4 (2.1)	8.6 (2.2)	10.8 (2.0)	7.3 (2.2)
CC _{1/2} (%)	99.8 (84.1)	99.7 (83.7)	99.9 (73.8)	99.0 (85.2)
Wilson <i>B</i> factor (Å ²)	23.5	23.2	27.5	26.2
Mosaicity (°)	0.05	0.05	0.13	0.26
Refinement statistics				
Resolution limits (Å)	93.3–2.10 (2.15–2.10)	93.2–2.20 (2.26–2.20)	93.4–2.20 (2.26–2.20)	93.08–2.90 (2.97–2.90)
<i>R</i> _{work} (%)	20.3 (25.1)	20.1 (24.9)	19.7 (27.7)	20.2 (28.5)
<i>R</i> _{free} (%)	24.5 (30.2)	24.9 (30.8)	24.5 (32.9)	26.8 (32.5)
No. reflections	90242 (6564)	78650 (5687)	78759 (5677)	34701 (1893)
No. test reflections	4830 (370)	4192 (307)	4203 (309)	2505 (137)
Model atoms	11635	11675	11642	11274
Protein <i>B</i> factor (Å ²)	37.2	37.4	40.3	62.3
Ligand <i>B</i> factor (Å ²)	26.9	24.6	27.9	41.2
r.m.s.d. bonds (Å)	0.007	0.008	0.008	0.007
r.m.s.d. angles (°)	1.27	1.29	1.28	1.25
Ramachandran plot				
Favoured (%)	97.6	97.4	97.4	96.0
Allowed (%)	2.3	2.5	2.5	3.2
Disallowed (%)	0.1	0.1	0.1	0.8
PDB code	5NVV	5NVW	5NVX	5NVY

Values in parentheses are for the highest resolution shell.

Dataset	Inhibitor 16	Inhibitor 17	Inhibitor 18	Inhibitor 19
Synchrotron	Diamond	Diamond	Diamond	Diamond
Wavelength (Å)	0.9282	0.9282	0.9282	0.9795
Processing statistics				
Space group	<i>P4₁22</i>	<i>P4₁22</i>	<i>P4₁22</i>	<i>P4₁22</i>
Unit cell parameters				
<i>a, b</i> (Å)	94.8	94.8	94.6	94.6
<i>c</i> (Å)	368.1	368.4	368.1	368.6
Resolution limits (Å)	49.6–2.70 (2.79–2.70)	49.6–2.30 (2.35–2.30)	49.5–2.10 (2.14–2.10)	49.5–2.20 (2.24–2.20)
Total reflections	355433 (35459)	580756 (35833)	626378 (25675)	772384 (41366)
Unique reflections	47321 (4567)	75814 (4421)	98140 (4785)	86260 (4448)
Completeness (%)	99.8 (99.9)	99.8 (99.9)	99.4 (99.9)	100 (100)
Multiplicity	7.5 (7.8)	7.7 (8.1)	6.4 (5.4)	9.0 (9.3)
<i>R</i> _{merge} (%)	13.2 (100.6)	8.8 (80.2)	6.6 (61.3)	12.0 (70.9)
<i>I</i> / σ (<i>I</i>)	11.9 (2.2)	15.0 (2.8)	14.8 (2.5)	11.0 (3.1)
CC _{1/2} (%)	99.9 (75.9)	99.9 (85.8)	99.9 (81.4)	99.8 (91.6)
Wilson <i>B</i> factor (Å ²)	36.0	34.6	33.2	31.1
Mosaicity (°)	0.18	0.06	0.05	0.05
Refinement statistics				
Resolution limits (Å)	94.8–2.70 (2.77–2.70)	94.8–2.30 (2.36–2.30)	94.6–2.10 (2.15–2.10)	94.6–2.20 (2.26–2.20)
<i>R</i> _{work} (%)	21.1 (31.4)	19.7 (22.9)	19.6 (25.4)	19.5 (22.6)
<i>R</i> _{free} (%)	27.0 (35.7)	23.8 (29.7)	23.8 (28.7)	24.2 (26.8)
No. reflections	44695 (3222)	71853 (5225)	93055 (6804)	81807 (5917)
No. test reflections	2419 (172)	3819 (286)	4964 (366)	4366 (321)
Model atoms	11069	11603	11697	11707
Protein <i>B</i> factor (Å ²)	52.8	47.7	44.5	42.4
Ligand <i>B</i> factor (Å ²)	41.3	39.2	33.5	29.8
r.m.s.d. bonds (Å)	0.007	0.007	0.007	0.008
r.m.s.d. angles (°)	1.22	1.21	1.25	1.27
Ramachandran plot				
Favoured (%)	96.1	97.6	96.1	96.1
Allowed (%)	3.9	2.3	3.6	3.9
Disallowed (%)	0	0.1	0	0
PDB code	5NVZ	5NWO	5NW1	5NW2

